Dynamic thermo-mechanical phenomena induced in isotropic cylinders impacted by high energy particle beams

A. Bertarelli & T. Kurtyka
CERN, European Organization for Nuclear Research, Switzerland

Abstract

High energy beams of elementary particles play a key role in laboratories working in fundamental research on particle physics. For several reasons (beam dump, secondary particle production etc.), these beams may be driven against solid structures. During such interactions, dynamic phenomena, very similar to those taking place after a mechanical impact, might occur in the hit solids. The studies of such dynamic thermo-mechanical problems are usually made via numerical methods. However, an analytical approach is also needed to provide reference solutions for the numerical results. In this paper a general introduction to these thermo-mechanical phenomena is first presented, followed by an example of the analytical solution for a graphite rod used as a beam target to produce secondary particles. The method allows the computation of the dynamic transient elastic stresses induced by a fast proton beam hitting off-axis the target. An exact solution for the temperature field is first obtained, using Fourier-Bessel series expansion. Quasi-static thermal stresses are then computed as a function of the calculated temperature distribution, making use of the thermoelastic displacement potential and of the Michell solution for the equivalent isothermal two-dimensional stress problem. Finally, the contribution of dynamic stresses due to longitudinal and bending stress waves is determined by means of the modal summation method, in the hypothesis of plane strain behaviour.
Keywords: Particle beams, particle impact, thermal stresses, dynamic thermal stresses.

Structures Under Shock and Impact VIII, N. Jones & C. A. Brebbia (Editors)

1 Introduction

1.1 High energy particle beams

CERN's purpose is to study the foundations of the structure of matter. Its sphere of activity is high energy physics, also known as elementary particle physics. Specifically, CERN designs, builds and operates high-energy accelerators and detectors.

In the accelerators are stored the particle beams which, circulating at relativistic energies, represent the main tool for CERN research.

These particle beams often interact with solids for several reasons: to clean the beam from the undesired particle halo surrounding the focused beam or absorb irregular beam losses (beam collimators), to create a barrier between different beam environments (vacuum, air and so on), to discharge the potentially highly destructive beam from the accelerator (beam dumps), to produce secondary particles via interaction with the atomic nuclei of the solids (beam targets). Beam targets are usually rods (though plates or cubes may also be found), which must safely undergo many rapid thermal cycles, without exceeding the elastic limit of the material. The analysis of the modes of failure of these components has shown that the wave and vibratory phenomena induced by thermal shocks play a very important role in the structural integrity.

1.2 Dynamic phenomena induced by thermal stress

When high energy particles interact with matter, thermal energy is produced inducing sudden temperature increase. This interaction is simulated from the energetic point of view with dedicated codes like FLUKA-2001. If the duration of the interaction is very short (of the order of milliseconds or less), the thermal expansion of the impacted material is partly prevented by its inertia. This gives birth to dynamic stresses propagating through the material with the velocity of sound as in structures hit by another solid.

These phenomena were studied by Bargmann [1] for the case of a uniformly rapidly heated rod on the basis of Laplace transforms and by Sievers [2] for thin rods and disks, making use of Fourier and Fourier-Bessel series with some particular boundary conditions. However, the analysis of more complicated cases is still necessary since the problem of non-uniform, non-axisymmetric heating was not solved. In fact, particle beams usually impact cylindrical targets in form of small spots, ideally concentric, but in practice always eccentric, because of mechanical misalignments. This induces also lateral oscillations leading in some cases to the collapse of the structure (Figure 1).

Usually these calculations, which involve nonlinearities coming from the temperature dependent properties of the material, are done using numerical methods (e.g. Finite Elements). Nevertheless, some preliminary estimations, to assess the degree of safety of the structure and to provide reference solutions, are largely needed. In this paper a method to evaluate quasi-static and dynamic stresses in a cylindrical rod, made of an ideally elastic material, is presented.

Structures Under Shock and Impact VIII, N. Jones & C. A. Brebbia (Editors)

Figure 1: Example of a metallic target rod bent and broken under the effect of transverse oscillations induced by a thermal shock.

2 Linear theory of thermoelasticity for an isotropic elastic body

2.1 Introduction

We consider the problem of linear thermoelasticity for the case of isotropic elastic solids. In the general expression of fully coupled thermoelasticity, the mechanical quantities depend upon the temperature field and vice versa.

Solids experience dilatational strains when subject to changes in temperature because of volumetric expansions. On the other hand, the rate of dilatational strain is a source of heat and hence of temperature changes.

The sets of equations governing linear thermoelasticity are derived from the general principles of thermodynamics (Nowacki [3], Boley and Weiner [4]). These relations represent the linear thermoelastic stress-strain relation (also known as the Duhamel-Neumann form of Hooke's law) (1), the equations of motion (2) and the heat conduction equation (3). In indicial notation, the stress-strain relation takes the following form:

$$\sigma_{ij} = \lambda \delta_{ij} \varepsilon_{kk} + 2\mu \varepsilon_{ij} - \delta_{ij} (3\lambda + 2\mu) \alpha (T - T_0) \quad (1)$$

where σ_{ij} and ε_{ij} are the components of the stress and strain tensor respectively, λ and μ are Lamé's constants, T is the temperature, T_0 is the temperature of a stress-free reference state, α is the coefficient of linear thermal expansion and δ_{ij} is the Kronecker delta.

When neglecting body forces, the equation of motion becomes:

$$\sigma_{ij,j} = \rho \ddot{u}_i \quad (2)$$

where ρ is the mass density and u_i are the components of the displacement vector. The wave equation can be obtained by introducing eqn (1) into eqn (2).

Structures Under Shock and Impact VIII, N. Jones & C. A. Brebbia (Editors)

Finally, the heat conduction equation, provided that the ratio $(T\text{-}T_0)/T_0$ is sufficiently small and no heat is generated in the reference volume, is given by:

$$kT_{,ii} = \rho c_E \dot{T} + (3\lambda + 2\mu)\alpha T_0 \dot{\varepsilon}_{kk} \tag{3}$$

where k is the thermal conductivity and c_E is the specific heat at constant deformation which in the present linear theory may be replaced by the specific heat at constant volume c_v.

2.2 Thermoelastic dissipation

In eqn (3), the mechanical coupling term is given by the last term on the right hand side of the equation. This term shows that a variation of strain is usually accompanied by variations in temperature and hence a flow of heat. Thus, the whole process gives rise to an increase of entropy. This phenomenon is known as thermoelastic dissipation and leads, in case of thermally excited dynamic phenomena, to what is known as thermoelastic damping. Many studies exist on this subject, but in this paper we will assume that the coupling term in eqn (3) is negligible as compared to the other terms and thus the temperature field is not affected by the variations of strain: this assumption gives birth to what is known as uncoupled thermoelastic theory.

According to Boley and Weiner [4] (on the basis of data from Goodier [5]), in the quasi-static case, this assumption is justified if it is verified that:

$$\delta << 1 \tag{4}$$

where δ is a nondimensional parameter given by

$$\delta = \frac{(3\lambda + 2\mu)^2 \alpha^2 T_0}{\rho^2 c_v v_e^{\,2}} \tag{5}$$

with the velocity of dilatational waves in an elastic medium being denoted by:

$$v_e = \sqrt{\frac{\lambda + 2\mu}{\rho}} \tag{6}$$

For graphitic materials eqn (4) is satisfied since δ is in the range of $3 \div 6x10^{-5}$, while for a steel it is between *0.01* and *0.02*.

If effects of inertia must be taken into account, satisfying eqn (4) might not be sufficient to neglect coupling. However, the same author has shown that in a predominantly unidirectional body, as the one of interest, the thermoelastic damping can be neglected on short time scales (*~1s*). Thus, the linear thermoelastic problem of rapid heating becomes a weakly coupled problem, in that the strain is influenced by the temperature distribution but not the inverse, making it much easier to treat.

3 The analytical approximate model

On the basis of the theory presented, an analytical model has been developed to study the thermomechanical dynamic response of isotropic rods to rapid thermal shocks. As an introductory example, this method is applied to a graphite rod used in the target station of the CNGS (*Cern Neutrino to Gran Sasso* facility), impacted by a proton beam. The CNGS experiment aims at obtaining a beam of neutrinos to be sent underground to a detecting station some 700 km away from CERN facilities (Elsener [6]).

The graphite cylindrical rod is simply supported at its extremities and is hit off-axis by two 400GeV proton bursts each lasting $t_{sp}=10\mu s$ with a separation of *50ms*. For this study we will focus only on the first pulse, assuming that the proton beam hits the cylinder parallel to the axis with a given eccentricity (Figure 2). It is assumed that the energy distribution induced by the beam is uniform along the *z*-axis and gaussian in the r-θ plane. Thanks to the assumption of weak coupling, the method can be outlined by the following sequential steps:

1. The uncoupled heat conduction equation is solved for $t>t_{sp}$ and the exact temperature distribution $T(r,\theta, t)$ is found (T is constant along the rod axis z).
2. Given $T(r,\theta, t)$, quasi-static stresses are calculated for the plane-strain case in two stages:
   a. Eqn (1) is solved not considering the boundary conditions.
   b. Boundary conditions are restored solving an ordinary isothermal elastic problem.
3. Axial dynamic stresses are calculated using the Modal Summation Method, via the application of two fictitious equivalent excitations at the rod extremities, induced by the quasi-static stress distribution.

The thermodynamic and mechanical properties of materials are in general temperature dependent, and this is taken into account in the numerical analyses; however to solve the problem analytically, we have assumed here some averaged values. This assumption permits also to assume $T_0=0$ as reference temperature, replacing T- T_0 with T.

More details on the method can be found in Bertarelli [7] and [8].

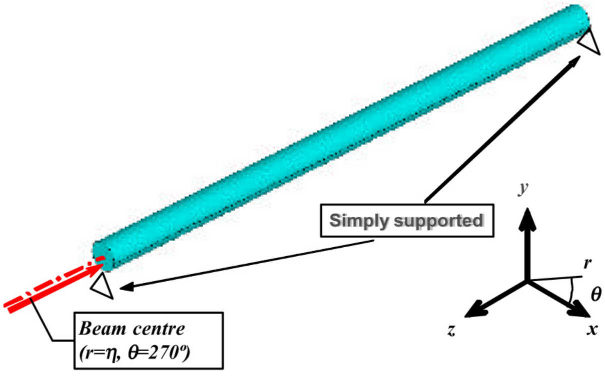

Figure 2: Target rod scheme and reference system. The rod length L is 100 *mm* and the radius R 2.5 *mm*. The beam hits the rod with a 1.5 *mm* eccentricity and has, at its centre, a maximum energy density U_{Max} of $8.61\times10^5\ J/kg$. The total deposited energy Q_T is *407 J* (i.e. $4.07x10^7$ *W* at a constant rate during *10 μs*).

Structures Under Shock and Impact VIII, N. Jones & C. A. Brebbia (Editors)

3.1 Thermal analysis

The temperature distribution is calculated from eqn (3), which, after removing the coupling term, becomes in polar coordinates:

$$\frac{\partial^2 T}{\partial r^2}+\frac{1}{r}\frac{\partial T}{\partial r}+\frac{1}{r^2}\frac{\partial^2 T}{\partial \theta^2}=\frac{1}{\kappa}\frac{\partial T}{\partial t} \tag{7}$$

To define the initial conditions we assume that during the impact time t_{sp} no diffusion process takes place and therefore the initial temperature distribution at $t=t_{sp}$ is simply given by:

$$T(r,\theta,t_{sp})=T_0(r,\theta)=\frac{U(r,\theta)}{c_v} \tag{8}$$

where $U(r,\theta)$ is the deposited energy per unit mass with gaussian distribution.

The boundary conditions are derived from the hypothesis of adiabatism, which can be retained thanks to the short duration of the phenomenon.

$$\frac{\partial T(R,\theta,t)}{\partial r}=0 \tag{9}$$

Making use of the Separation of Variable method, and expressing the initial condition as a Fourier series whose nth harmonic term (cosine or sine) is $H_n(\theta)$, we can obtain the solution in the following form:

$$T(r,\theta,t)=\sum_n\sum_s C_{n,s}J_n(\lambda_{n,s}r)e^{-\kappa\lambda_{n,s}{}^2 t}H_n(\theta) \tag{10}$$

where J_n is a Bessel function of the first kind of order n, $C_{n,s}$ are numerical coefficients obtained from the initial condition (8) and $\lambda_{n,s}$ are the eigenvalues of the problem obtained by the application of the adiabatic condition (9).

The analysis of the solution shows that the time necessary to reach thermal equilibrium is of the order of *0.4s*. This confirms that the time scale of interest is actually limited to some tenths of second.

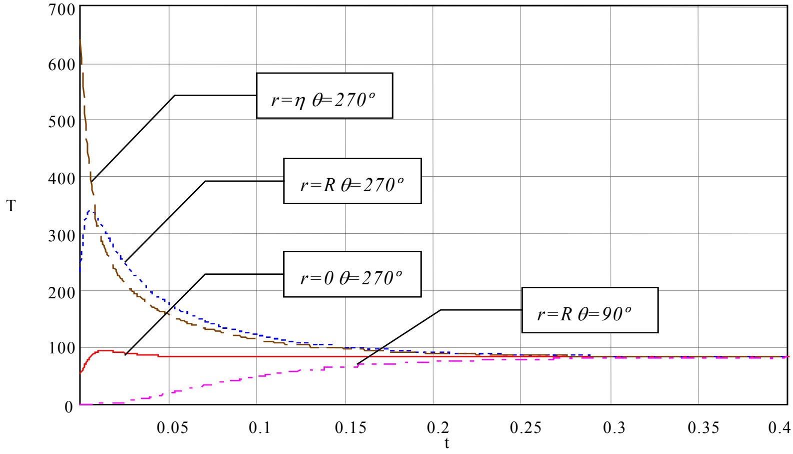

Figure 3: Temperature as a function of time at various locations.

3.2 Quasi-static analysis

Quasi-static stresses can be obtained by adapting a method developed by Goodier [9], [10], applied to the plane-strain case (hypothesis of a long cylinder) assuming that longitudinal expansion is prevented.

Stresses are calculated from the superposition of two contributions: *(i)* stress components arising from a *displacement potential* $\psi(r, \theta, t)$ satisfying the thermoelastic stress-strain relation (1) with the given temperature distribution $T(r, \theta, t)$, but not the mechanical boundary conditions (free-boundary) and *(ii)* stress components due to pressure loads applied isothermally on the outer surface of the cylinder, to restore the free-boundary condition.

From the displacement potential, the two in-plane displacement components can be obtained, with the *z*-component identically zero.

The strain components are then obtained from the well-known kinematic relations in polar coordinates (Timoshenko and Goodier [10]); the stress components $\overline{\sigma}'_r$, $\overline{\sigma}'_\theta$ and $\overline{\tau}'_{r\theta}$ are subsequently calculated making use of eqn (1) with $\overline{\varepsilon}'_z = 0$.

To restore the correct boundary conditions, we add on the rod surface a pressure distribution removing non-zero forces. To do so, we make use of the Michell's expression of the *Airy's stress function* $\phi(r, \theta, t)$ applied to the ordinary plane-strain problem [10]. Once $\phi(r, \theta, t)$ is known, stress components $\overline{\sigma''_r}, \overline{\sigma''_\theta}$, and $\overline{\tau''_{r\theta}}$ can be calculated in the usual way.

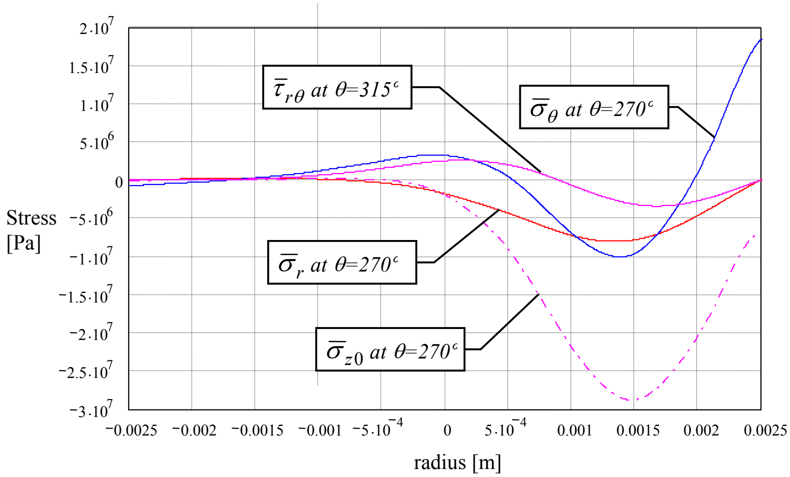

Figure 4: Quasi static stresses at $t=t_{sp}$ as a function of radius and angle.

Quasi static stresses at zero axial strain (Figure 4) are found by summing components from the two contributions. Axial stress is always negative having assumed that axial expansion is prevented.

All these stress components tend to disappear as the temperature distribution becomes uniform.

3.3 Dynamic analysis

Numerical analyses (Bertarelli [7]) have shown that for cylindrical rods the contribution of radial waves over stresses is almost negligible. Therefore we will focus our dynamic analysis on the study of longitudinal and bending oscillations, neglecting the presence of radial waves. The same assumption also allows us to ignore the effect of transversal contraction due to Poisson's ratio, hence we can replace eqn (6) for v_e with $\sqrt{E/\rho}$. For in-plane total stresses, the quasi-static values of $\overline{\sigma}_r$, $\overline{\sigma}_\theta$ and $\overline{\tau}_{r\theta}$ will be retained.

Instead of trying to solve explicitly the equations of motion (2), we resort to the modal analysis, studying separately the response of the rod to two fictitious excitations linearly rising from zero in t_{sp}, represented by the equivalent axial force F_z and the bending moment M_x applied at the extremities of the rod.

These two actions are necessary to ensure the equilibrium at the free extremities of the rod. The axial force and moment can be calculated as the opposite of the resultants of the axial quasi-static stress $\overline{\sigma}_{z0}$.

The equivalent axial force is obtained via the following integral:

$$F_z(t) = -2\int_{-\pi/2}^{\pi/2}\int_0^R \overline{\sigma}_{z0}(t) r dr d\theta \tag{11}$$

It can be shown ([7], [8]) that for $t \geq t_{sp}$, F_z remains constant and is proportional to the total deposited energy Q_T or, which is the same, to the final uniform temperature T_f:

$$F_z = \frac{E\alpha Q_T}{c_v \rho L} = E\alpha T_f \pi R^2 \quad \text{for } t \geq t_{sp} \tag{12}$$

Hence the effect of $F_z(t)$ is equivalent to a fictitious excitation linearly rising from zero up to a constant value in a time t_{sp} (Figure 5).

With eccentricity measured along the vertical axis, the equivalent bending moment about horizontal axis M_x can be computed likewise.

In this case the resultant always depends upon time and becomes zero when $t \to \infty$, as one could expect, since temperature gradient disappears. Anyhow, it is interesting to note that M_x initially tends to decrease linearly. Therefore its dynamic effect can be approximately represented by an excitation rising from zero to a maximum in t_{sp} and then linearly decreasing to zero in a convenient time (Figure 5).

To calculate the time-response we make use of the Modal Summation Method (Thomson [11]), which basically expands the deformation in terms of the *normal modes* $\phi_{zi}(z)$ or $\phi_{fi}(z)$ and of the *generalized coordinates* $q_{zi}(t)$ or $q_{fi}(t)$ of a simply supported uniform beam loaded at the extremities with $F_z(t)$ or $M_x(t)$ respectively. The equation of motion for each linearly independent mode is obtained by the application of the Lagrange equation.

As the generalized forces and the natural modes and frequencies for a simply supported beam are known, the generalized coordinates $q_{zi}(t)$ or $q_{fi}(t)$ can be calculated from the response of a single-DOF system to a generalized force with a time history $g(t)$ or $g'(t)$ respectively (Figure 5) and thus the lateral and

Structures Under Shock and Impact VIII, N. Jones & C. A. Brebbia (Editors)

longitudinal displacements obtained. Hence, one can finally calculate the dynamic components of axial stress and superimpose them to the quasi static component to obtain the total axial stress σ_z (Figure 6).

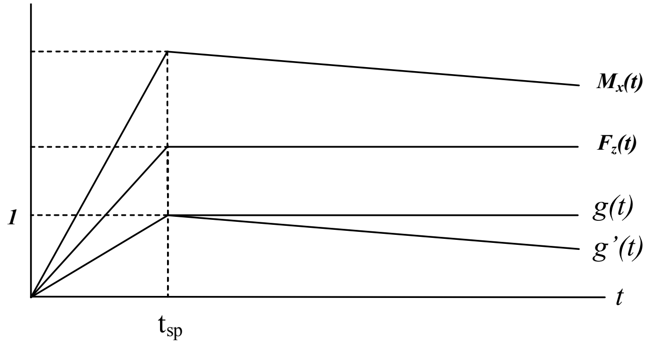

Figure 5: Equivalent dynamic excitations acting on the rod extremities.

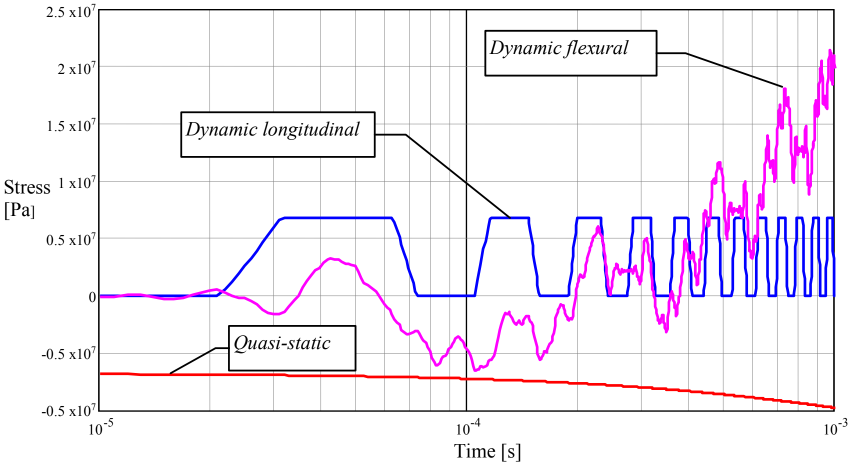

Figure 6: Quasi-static and dynamic components of axial stress at $r=R$, $\theta=270°$.

In Figure 7 total axial stress on the outer surface of the rod at $\theta=270^o$ is shown: the effect of the different components can be identified. The compressive quasi-static stress at zero strain is the only component initially present; then, the longitudinal waves start to build up assuming a trapezoidal shape with a maximum amplitude constant in time as shown in Figure 6.

The dynamic longitudinal stress induced by the positive fictitious excitation $F_z(t)$ oscillates between 0 and $2F_z/\pi R^2$. This has a simple physical explanation: two equal longitudinal waves with amplitude $\varepsilon_z = F_z/E\pi R^2$ depart from the rod ends travelling at the speed of sound v_e, superimposing each other along the

Structures Under Shock and Impact VIII, N. Jones & C. A. Brebbia (Editors)

rod with positive or negative sign according to their direction. Hence the period T_{zl} of each oscillation is given by $T_{zl} = 2L/v_e = 84\mu s$ and the corresponding frequency f_{zl} is *11.9 kHz*.

The bending term due to the lateral oscillations induced by the equivalent excitation $M_x(t)$ starts to appear much later but its effect becomes then predominant, leading to a bending stress as much as three times larger than the corresponding static stress. Its fundamental period T_{zf} is *2.1 ms* and its frequency f_{zf} is *467 Hz*.

The total axial stress neglecting inertia effects is also plotted in Figure 7. It is obtained by adding to the zero-strain quasi-static axial stress, the static contributions due to $F_z(t)$ and $M_x(t)$.

The comparison clearly indicates that the dynamic effects are very important: the highest dynamic total stress is more than three times larger than the maximum quasi-static axial stress. The peak stress is found much after the initial impact, at about *1 ms*.

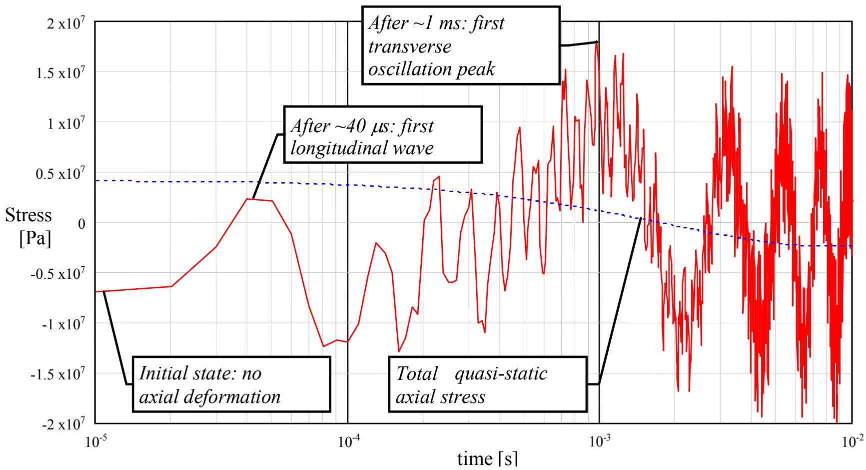

Figure 7: Total axial stress as a function of time at $r=R$, $\theta=270^o$.

4 Conclusions

In this paper the mechanical response of a graphite isotropic cylindrical rod rapidly heated by an intense high-energy proton beam was studied. Quasi-static stresses and total axial stress, including dynamic effects, were determined analytically in the hypothesis of ideal elastic behaviour and plane-strain deformation. Results show that the thermal shock, on top of quasi static stresses, gives birth to two main dynamic phenomena: axial stress waves travelling at the speed of sound along the rod, with intensity proportional to the total deposited energy and transversal vibrations arising when the rod is hit off-axis by the beam. These vibrations induce bending stresses that are much higher than the quasi-static stresses generated by the non uniform temperature distribution; in addition, the peak bending stress occurs much after the initial impact has taken place. Hence, each time a thermal shock occurs on a slender structure, the induced dynamic phenomena cannot be neglected and must be carefully analysed for a relatively extended time as compared to the duration of the impact.

References

[1] Bargmann, H., *Dynamic Response of External Targets under Thermal Shock,* Technical Note LAB II/BT/Int./73-3, CERN, Geneva, 1973.

[2] Sievers, P., *Elastic Stress Waves in Matter Due to Rapid Heating by an Intense High-energy Particle Beam,* Technical Note LAB II/BT/74-2, CERN, Geneva, 1974.

[3] Nowacki, W., *Thermoelasticity,* Pergamon Press, Oxford, 2nd ed. 1983.

[4] Boley B.A., Weiner, J.W., *Theory of Thermal Stresses,* John Wiley & Sons, New York, 1960.

[5] Goodier, J.N., Thermal Stress and Deformation, *Journal of Applied Mechanics*, **24(3)**, 467-471, 1957.

[6] Elsener, K., *General Description of the CERN Project for a Neutrino Beam to Gran Sasso (CNGS),* CERN AC note 2000-03, CERN, Geneva, 2000.

[7] Bertarelli, A., *Analytical Study of Axisymmetric Transient Thermal Stresses in Graphite Target Rods for the CNGS Facility*, Technical Note EST-ME 2003-005, CERN, Geneva, 2003.

[8] Bertarelli, A., *An Analytical Model to study Transient Thermal Stresses in Graphite Target Rods hit by Off-axis beam for CNGS Facility,* Technical Note EST-ME 2003-06, CERN, Geneva, 2003.

[9] Goodier, J.N., On the Integration of the Thermo-elastic Equations, *Phil. Mag. (seventh series),* **23**, 1017-1032, 1937.

[10] Timoshenko, S. P., Goodier, J. N., *Theory of Elasticity*, McGraw-Hill, NewYork, 3rd ed. 1970.

[11] Thomson, W.T., *Theory of Vibration with Applications*, Chapman & Hall, London, 4th ed. 1993.

Structures Under Shock and Impact VIII, N. Jones & C. A. Brebbia (Editors)